Emergence of Slow Collective Oscillations in Neural Networks with Spike-Timing Dependent Plasticity

Kaare Mikkelsen,[1,*] Alberto Imparato,[1,†] and Alessandro Torcini[2,3,1,‡]

[1]*Department of Physics and Astronomy, University of Aarhus, Ny Munkegade, Building 1520, DK-8000 Aarhus C, Denmark*
[2]*CNR-Consiglio Nazionale delle Ricerche-Istituto dei Sistemi Complessi, via Madonna del Piano 10, I-50019 Sesto Fiorentino, Italy*
[3]*INFN Sezione di Firenze, via Sansone, 1-I-50019 Sesto Fiorentino, Italy*

The collective dynamics of excitatory pulse coupled neurons with spike-timing dependent plasticity is studied. The introduction of spike-timing dependent plasticity induces persistent irregular oscillations between strongly and weakly synchronized states, reminiscent of brain activity during slow-wave sleep. We explain the oscillations by a mechanism, the Sisyphus Effect, caused by a continuous feedback between the synaptic adjustments and the coherence in the neural firing. Due to this effect, the synaptic weights have oscillating equilibrium values, and this prevents the system from relaxing into a stationary macroscopic state.

PACS numbers: 05.45.Xt, 87.19.lm, 87.19.lw, 87.19.lj

Sisyphus was the mythological king of Corinth compelled to roll a heavy boulder up a hill, only to watch it roll back down as it approached the top. Sisyphus was condemned by Zeus for his iniquity and pride to repeat eternally his efforts, without any hope of success. However, in the brain, such endless motion can have a positive functional relevance. Fluctuating spontaneous activity has been observed in several areas of the brain [1]. In particular, irregular oscillations between more and less synchronized states have been revealed in the hippocampus during slow-wave sleep and this activity has been related to memory consolidation in the neocortex [2].

Recent studies have suggested synaptic plasticity as a fundamental ingredient to ensure multistability in neuronal circuits [3–6]. In particular, spike-timing dependent plasticity (STDP) is considered one of the central mechanisms underlying information elaboration and learning in the brain [7]. A series of experiments performed *in vivo* and *in vitro* on neural tissues revealed that the strength of a synapse, conveying spikes from a presynaptic to a postsynaptic neuron, depends crucially on the precise spike timing of the two connected neurons [8–10]. The STDP rules prescribe that whenever the presynaptic (postsynaptic) neuron fires before the postsynaptic (presynaptic) one, the synapse is potentiated (depressed). The synapse is modified only if the spikes occur within certain time intervals (*learning windows*). Asymmetric learning windows have repeatedly been found experimentally (e.g., see Refs. [11–13]). This asymmetry is a prerequisite, at least in phase oscillator networks, to observe the coexistence of states characterized by different levels of synchrony [3,4]. Furthermore, in the presence of propagation delays STDP can provide a negative feedback mechanism contrasting highly synchronized network activity and promoting, in randomly driven networks, the emergence of states at the border between randomness and synchrony [5].

In this Letter, a novel deterministic mechanism, the *Sisyphus effect* (SE), able to generate spontaneous fluctuations in a neural network between asynchronous and synchronous regimes is presented. In particular, we study excitatory pulse coupled neural networks with STDP, where the interaction among neurons is mediated by α pulses [14]. For nonplastic interactions, the excitatory coupling leads to synchronization only for sufficiently fast synapses [15]. Furthermore, the desynchronizing effect is amplified at large coupling [16]. In absence of plasticity, the macroscopic activity of the network is stationary: asynchronous for large synaptic weights and partially synchronized for sufficiently weak coupling [16,17].

The introduction of STDP completely modifies the dynamical landscape leading to a regime where a strongly and a weakly synchronized state coexist. The activity of the network is, thus, characterized by irregular oscillations between these two states. These transitions are driven by the evolution of the synaptic weights, which in turn is dictated by the level of synchrony in the network. For small synaptic weights, the system is fully synchronized, while above a critical coupling it desynchronizes. Furthermore, whenever the network is synchronized (desynchronized) the synaptic weights tend towards large (small) equilibrium values corresponding to asynchronous (synchronous) dynamics. In summary, the neuronal activity can be represented in terms of an order parameter diffusing over an effective free energy landscape displaying two coexisting equilibrium states. Small (large) synaptic weights tilt the landscape towards the strongly (weakly) synchronized state; in turn, the induced activity increases (reduces) the weights until a tilt in the opposite direction occurs. Thus, the landscape oscillates endlessly.

The model.—We study a fully coupled network of N leaky integrate-and-fire neurons, for which the membrane potential $V_i(t) \in [0{:}1]$ of neuron i evolves as:

$$\dot{V}_i(t) = a - V_i(t) + I_i(t), \qquad i = 1, \ldots, N, \qquad (1)$$

whenever the neuron reaches the threshold $V_i = 1$, an α pulse $p_\alpha(t) = \alpha^2 t \exp(-\alpha t)$ is instantaneously transmitted to all other neurons and V_i is reset to zero. Furthermore, $a > 1$ is the suprathreshold dc current, $I_i = g E_i$ the synaptic current, and g the excitatory *homogeneous* coupling. The field E_i represents the linear superposition of the pulses received by neuron i and its evolution is ruled by a second order differential equation [Eq. (S2) in Ref. [18]]. For a fully coupled nonplastic network the synaptic weights associated to the connection from the presynaptic jth neuron to the postsynaptic ith one are $w_{ij} = 1$ (apart from the autaptic terms: $w_{ii} = 0$).

In the presence of plasticity, we assume that the weights evolve in time according to a *nearest-neighbor* STDP rule with soft bounds [4,7,19–21]. Therefore, in the case of a post- (presynaptic) spike, emitted by neuron i (j) at time t, the weight w_{ij} is potentiated (depressed) as $w_{ij}(t^+) = w_{ij}(t^-) + \Gamma_{ij}(t)$, with

$$\Gamma_{ij}(t) = \begin{cases} p[w_M - w_{ij}(t^-)]e^{-(\delta_{ij}/\tau_+)} & \text{if } \delta_{ij} > 0 \\ -dw_{ij}(t^-)e^{+(\delta_{ij}/\tau_-)} & \text{if } \delta_{ij} < 0, \end{cases} \quad (2)$$

where $\delta_{ij} = t - t^{(j)} > 0$ ($\delta_{ij} = t^{(i)} - t < 0$) is the firing time difference and $t^{(k)}$ the last firing time of neuron k. The potentiation and depression factors (p and d, respectively) coincide, unless otherwise specified [22]. The bounds keep the synapses from achieving unrealistically large values or becoming inhibitory, namely $0 \leq w_{ji} \leq w_M$. The learning windows over which post- (pre-) synaptic spikes will cause synaptic potentiation (depression) are indicated as τ_+ (τ_-). Following experimental evidences [11], we assume $\tau_- > \tau_+$. The degree of synchronization of the neurons is measured by the order parameter [23,24] $R(t) = |(1/N)\sum_k e^{i\theta_k(t)}|$, where $\theta_k(t) = 2\pi(t - t_m^{(k)})/(t_{m+1}^{(k)} - t_m^{(k)})$ is the phase of the kth neuron at time t between its mth and $(m + 1)$th spike emission. A perfectly synchronized (asynchronous) system has $R = 1$ ($R = 0$), while intermediate values indicate partial synchronization.

Phase diagram.—We analyze how the phase diagram of the network is modified by the plasticity. In particular, we focus on the variation of the neuronal coherence by varying the dc current. Similar results can be obtained by varying the coupling g and the pulse width α (as shown in [18]). To compare with previous results obtained without plasticity, we fix $g = 0.4$ and $\alpha = 9$ as in [17,25]. In absence of plasticity, the homogeneous system exhibits two phases: an asynchronous regime with $R \equiv 0$, and a partially synchronized phase with finite R [17]. The emergence of one or the other regime depends crucially on the ratio of two time scales: the pulse rise time $1/\alpha$ and the interspike-interval (ISI) [15,25]. For slow synapses (relative to the ISI) the system dynamics is asynchronous, while for sufficiently fast synapses coherent oscillations emerge. The system
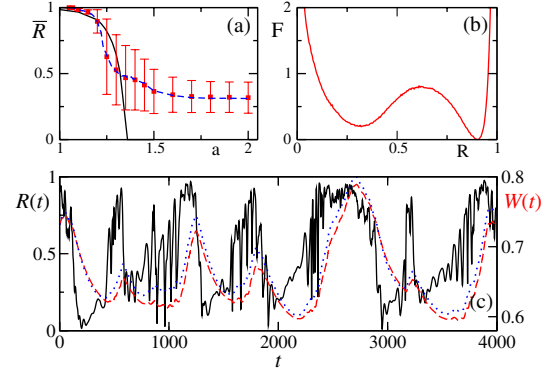

FIG. 1 (color online). (a) Average order parameter $\bar{R}$ as a function of a for the nonplastic network (black solid line) and in the presence of STDP for $N = 200$ (red filled squares) and $N = 500$ (blue dashed line). (b) Free energy profile $F(R)$ versus R for $N = 200$, obtained by evaluating R at regular time intervals $\Delta t = 1$ for a time span $\sim 5 \times 10^6$. (c) Time evolution of $R(t)$ (black solid line) and of $W(t)$ (red dashed line) for $N = 500$. The dotted (blue) line is the W predicted via Eq. (3). The data refer to $a = 1.3$, $g = 0.4$, $\alpha = 9$, $d = p = 0.01$, $\tau_- = 3\tau_+ = 0.3$, and $w_M = 2$, and are measured after a transient $\sim 10^5$.

becomes fully synchronized only for instantaneous synaptic rise times (i.e., $\alpha \rightarrow \infty$). For fixed network size N and pulse shape, the ISI can be reduced by increasing either the external dc current or the synaptic coupling. Therefore, partial synchronization is observable for sufficiently small a or g values (whenever $\alpha \gtrsim 3.4$), while incrementing these parameters will desynchronize the system [16] [as shown in Fig. 1(a) in [18]].

The average level of synchronization $\bar{R}$ is reported in Fig. 1(a) as a function of a for the nonplastic and plastic cases. In absence of plasticity, the system is partially synchronized for low dc currents and asynchronous for $a \geq a_c \simeq 1.35$. The introduction of plasticity does not alter the scenario at small a values, where the system is in a *high synchronization* (HS) regime. The main difference is observable in the dynamics of $R(t)$, which displays irregular oscillations: the associated Fourier spectrum resembles a Lorentzian with a small subsidiary peak around period $\simeq 34$–36. However, for sufficiently large currents, namely $a > 1.5$, the asynchronous regime is substituted by a state of *low synchronization* (LS) characterized by a rapidly fluctuating order parameter (over a time scale of the order of 70–150) with an associated small level of synchronization $\bar{R} \simeq 0.32 \pm 0.12$. At intermediate a values, in the range $a \in [1.23; 1.46]$, R exhibits wide irregular temporal oscillations between values $\simeq 1$ and zero with characteristic time scales $\simeq 1100$–1400. These latter oscillations represent low frequency fluctuations (LFFs), while rapid fluctuations are still present over time scales $\simeq 50$–60 [see Fig. 1(c)].

In this Letter, we will mainly focus on the intermediate regime, fixing $a = 1.30$, where the LFF of $R(t)$ resembles the evolution of a particle in a double well potential subject

to thermal fluctuations. To clarify this analogy, we have estimated the probability distribution function (PDF), $P(R)$, of the order parameter, by examining its trajectory for a sufficiently long time span, and derived the associated *free energy* profile as $F(R) = -\log P(R)$. As shown in Fig. 1(b), $F(R)$ exhibits two minima corresponding to a HS phase at $R_H \simeq 0.905$ and a LS state at $R_L \simeq 0.32$. The 2 coexisting minima are separated by a saddle, located at $R_S \simeq 0.61$. As clarified in the following the jumps between minima are driven by the macroscopic evolution of network plasticity. The rapid fluctuations, present in all regimes, are instead due to the microscopic evolution of the synaptic weights, which can be interpreted as a noise source for the dynamics of $R(t)$. The analysis of these *noise-induced oscillations* goes beyond the scope of this Letter and it is left for future studies.

Constrained phase diagram.—As shown in Fig. 1(c), the LFFs of $R(t)$ are associated with oscillations in the average synaptic weight $W(t) \equiv \sum_{i,j} w_{ji}(t)/N(N-1)$. In particular, when the system is in a HS (LS) state W increases (decreases).

To better investigate the origin of these correlations and the interaction between the STDP induced synaptic dynamics and the level of synchronization in the system, we perform the following numerical experiments. We simulate the system by constraining the synaptic weights to have a constant average value W_0, by rescaling, at regular time intervals, the weights w_{ij}. Initially, $W_0 = 0$ and we follow the evolution of the system for a time span T_S. We then perform a new simulation for the same time lapse with a larger W_0 value, starting from the last configuration of the previous run. The procedure is repeated by increasing W_0 at regular steps ΔW_0 until $W_0 = w_M$ is reached. Then, with the same protocol, W_0 is decreased (in steps of ΔW_0) until finally W_0 returns to zero [26]. The results of these simulations are shown in Fig. 2 for $N = 200$. At low W_0 the system is fully synchronized, while with increasing W_0, the system desynchronizes via a discontinuous transition. By further increasing W_0 the level of synchronization continues to decrease and another smooth transition seems to occur. For the explanation of the SE, it is sufficient to limit the analysis to the first transition.

As shown in Fig. 2, the constrained system exhibits a hysteretic transition from HS to LS (from LS to HS) for $W_0^{(1)} = 0.76(5)$ [$W_0^{(2)} = 0.65(5)$] by increasing (decreasing) the control parameter W_0 [27]. This implies that in the interval [$W_0^{(2)}, W_0^{(1)}$] the two regimes coexist and that HS or LS is observable depending on the initial state of the network.

Mean field synaptic evolution.—In order to gain some insight into the evolution of the system during unconstrained simulations (USs), let us consider a mean field equation for the synaptic weight evolution. The average synaptic weight modification Γ, for each presynaptic spike, can be written as [19]
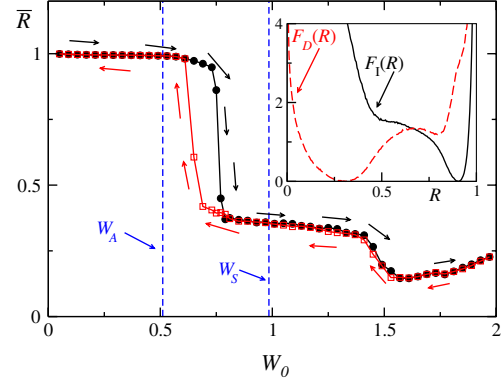

FIG. 2 (color online). $\bar{R}$ versus W_0 as measured for increasing (black filled circles) and decreasing (empty red squares) W_0. The (blue) vertical dashed lines indicate the fixed point values W_S and W_A [18]. Results averaged over 8 different initial conditions, $T_S = 1000$, $\Delta W_0 = 0.02$ (for clarity only one point every two is shown). (Inset) Conditional free energy profiles $F_I(R)$ (black solid line) and $F_D(R)$ (red dashed line) obtained during USs. Both curves are vertically shifted to achieve zero as minimal value. Parameters as in Fig. 1 and $N = 200$.

$$\Gamma(t) = p(w_M - W) \int_0^\infty d\delta P(\delta) e^{-\delta/\tau_+}$$
$$- dW \int_{-\infty}^0 d\delta P(-\delta) e^{\delta/\tau_-}, \qquad (3)$$

where $P(\delta)$ is the PDF of the time differences δ between postsynaptic and presynaptic firing measured. To test the predictive value of Eq. (3), we have measured from an US $P(\delta)$ at regular intervals Δt. By employing this information we can predict quite well the evolution of the synaptic weight as $W(t + \Delta t) = W(t) + \Gamma(t)$ [see Fig. 1(c)].

By assuming that the postsynaptic neuron is firing with period T_0, we are able to derive the time difference distribution $P(\delta)$ for the two limiting cases: fully synchronized and asynchronous dynamics. In the fully synchronized (asynchronous) situations, we expect a distribution of the form $P_S(\delta) = \mathcal{D}(\delta) + \mathcal{D}(\delta - T_0)$ ($P_A(\delta) = 1/T_0$) defined in the interval [0:T_0]. Here $\mathcal{D}$ denotes a Dirac delta function. These guesses are essentially confirmed by direct USs as shown in Fig. 3 in [18]. Therefore, in these two cases, an analytical estimation of Γ can be obtained. Furthermore, in both cases, Γ vanishes for a finite value of the average synaptic weight, namely W_S (W_A) for the synchronized (asynchronous) situation. Furthermore, for $W < W_S$ ($W > W_S$) the synapses are on average potentiated (depressed). The same occurs in the asynchronous case for $W < W_A$ ($W > W_A$). This implies that W_S (W_A) is a stable attractive point for the dynamics of W in the synchronized (asynchronous) regime [for a definition of W_S and W_A see Eq. (S8) and (S10) in [18]].

Sisyphus mechanism.—We are now able to explain the behavior reported in Fig. 1(c) for $R(t)$ and $W(t)$. Let us suppose that the system is in the HS phase with an
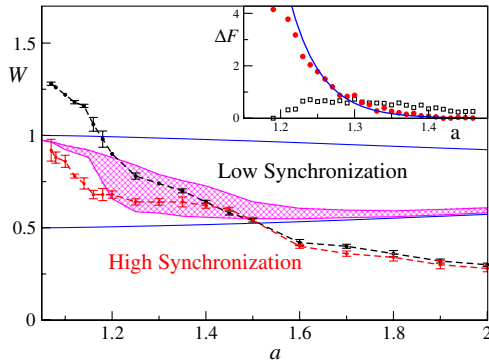
FIG. 3 (color online). W versus the dc current a. The shaded
area represents the W values measured during USs. The upper
black (lower red) dashed line refers to the estimated $W_0^{(1)}$ ($W_0^{(2)}$).
The error bars have been evaluated over 5 different realizations
of the constrained simulations. The upper (lower) solid blue line
represents the fixed point values W_S (W_A). (Inset) The red circles
(black squares) refer to the free energy barrier ΔF separating
the HS (LS) state from the saddle. The blue line is an exponential
fit to the HS barrier height. The remaining parameters as in
Fig. 1 and $N = 500$.

associated low coupling $W < W_0^{(1)}$. However, in this situ-
ation, the attractive fixed point W_S is above the transition
point $W_0^{(1)}$ (see Fig. 2). Therefore, W keeps increasing, until
for $W > W_0^{(1)}$ the system starts to desynchronize and to
approach the LS state. In this phase, the $P(\delta)$ becomes
almost flat [see Fig. 3(b) in [18]] and the attractive point
for the synaptic evolution will be W_A, located below $W_0^{(2)}$.
The motion towards W_A leads to a decrease of W. Whenever
the average synaptic weight crosses $W_0^{(2)}$, the neurons begin
to resynchronize. Finally, the system will return to the HS
state from where it started. The cycle will repeat indefi-
nitely and is the essence of the SE.

The above arguments are approximate because the sys-
tem is never exactly fully synchronized or desynchronized,
instead it passes through a continuum of states, each
associated to a different fixed point in W space. The
relevant aspect is that the fixed points associated to the
HS (LS) phase are larger than the transition point $W_0^{(1)}$
(smaller than $W_0^{(2)}$). As we have verified this is indeed the
case, therefore, the mechanism is still valid. To perform a
direct test of the validity of our analysis, we have measured
the PDF of R conditioned to the fact that W was increasing
(decreasing) during an US. From these PDFs we derived
the corresponding free energy profile $F_I(R)$ ($F_D(R)$).
As shown in the inset of Fig. 2, F_I has a unique minimum
at R_H, while F_D has an absolute minimum at R_L and a
shoulder around $R \simeq 0.8$. These results confirm that the
equilibrium attractive values for W are located opposite
to the transition points, because when the system is in the
HS (LS) regime the synaptic weights increase (decrease)
continuously trying to reach the corresponding fixed
points.

The SE should be active whenever the transition values
$W_0^{(1)}$ and $W_0^{(2)}$ are both contained within the interval
$[W_A, W_S]$. To verify this statement we have measured
$W_0^{(1)}$, $W_0^{(2)}$ and the fixed points for various dc currents
within the interval $0 < a \leq 2$ (data shown in Fig. 3).
We observe that the transition is hysteretic in the interval
$a \in \ ]0; 1.40]$, while for larger values, $W_0^{(1)}$ and $W_0^{(2)}$ es-
sentially coincide. Furthermore, $W_0^{(1)}$ becomes larger than
W_S at $a \simeq 1.18$, while $W_A \geq W_0^{(1)}$, $W_0^{(2)}$ for $a \geq 1.50$.
Thus, we expect that $F(R)$ exhibits two coexisting minima,
due to the SE, when $1.18 \leq a \leq 1.50$. To verify this con-
jecture, we estimate the free energy barrier heights ΔF
separating the HS and the LS state from the intermediate
saddle for various a values. As shown in the inset of Fig. 3,
the barrier associated to the HS state diverges exponen-
tially when approaching $a \simeq 1.18$. Therefore, the HS
regime is only possible at smaller a values. On the other
hand, the two minima merge and the associated barriers
vanish for $a \geq 1.48$ indicating that the LS state is unique
remaining at large a. Furthermore, the distributions of the
W values measured during USs are reported in Fig. 3 as a
shaded area: these values include the transition interval
$[W_0^{(1)}; W_0^{(2)}]$ for $1.20 \leq a \leq 1.48$.

In conclusion, the SE should be observable in pulse
coupled neural networks whenever the excitation has a
desynchronizing effect. This is, in general, verified for
any kind of neuronal response (type I or type II) for suffi-
ciently slow synaptic interactions [15,16]. Furthermore,
we have verified that the SE persists by setting $p > d$, as
suggested by experimental evidences [13].

*kbm05@phys.au.dk
†imparato@phys.au.dk
‡alessandro.torcini@cnr.it

[1] K. D. Harris and A. Thiele, Nat. Rev. Neurosci. **12,** 509
(2011).
[2] G. Buzsáki, Neuroscience (N.Y.) **31,** 551 (1989).
[3] P. Tass and M. Majtanik, Biol. Cybern. **94,** 58 (2006).
[4] Y. L. Maistrenko, B. Lysyansky, C. Hauptmann, O.
Burylko, and P. A. Tass, Phys. Rev. E **75,** 066207 (2007).
[5] E. V. Lubenov and A. G. Siapas, Neuron **58,** 118 (2008).
[6] G. Mongillo, D. Hansel, and C. van Vreeswijk, Phys. Rev.
Lett. **108,** 158101 (2012).
[7] J. Sjöström and W. Gerstner, Scholarpedia **5,** 1362 (2010).
[8] H. Markram, J. Lübke, M. Frotscher, and B. Sakmann,
Science **275,** 213 (1997).

[9] J. C. Magee and D. Johnston, Science **275**, 209 (1997).

[10] G. Q. Bi and M. M. Poo, J. Neurosci. **18**, 10 464 (1998).

[11] G. Q. Bi and M. M. Poo, Annu. Rev. Neurosci. **24**, 139 (2001).

[12] G. Q. Q. Bi and H. X. X. Wang, Physiol. Behav. **77**, 551 (2002).

[13] R. Froemke and Y. Dan, Nature (London) **416**, 433 (2002).

[14] L. F. Abbott and C. van Vreeswijk, Phys. Rev. E **48**, 1483 (1993).

[15] C. Vreeswijk, L. F. Abbott, and G. B. Ermentrout, J. Comput. Neurosci. **1**, 313 (1994).

[16] D. Hansel, G. Mato, and C. Meunier, Neural Computation **7**, 307 (1995).

[17] C. van Vreeswijk, Phys. Rev. E **54**, 5522 (1996).

[18] See Supplemental Material at http://link.aps.org/supplemental/10.1103/PhysRevLett.110.208101 for more details on the model, on the phase diagrams, on the $P(\delta)$, and on the fixed point solutions for W.

[19] E. M. Izhikevich and N. S. Desai, Neural Comput. **15**, 1511 (2003).

[20] C. C. Chen and D. Jasnow, Phys. Rev. E **81**, 011907 (2010).

[21] C. C. Chen and D. Jasnow, Phys. Rev. E **84**, 031908 (2011).

[22] All the quantities appearing in the model are dimensionless.

[23] A. Winfree, *The Geometry of Biological Time* (Springer-Verlag, Berlin, 1980).

[24] Y. Kuramoto, *Chemical Oscillations, Waves, and Turbulence*, Dover Books on Chemistry Series (Dover Publications, New York, 2003).

[25] R. Zillmer, R. Livi, A. Politi, and A. Torcini, Phys. Rev. E **76**, 046102 (2007).

[26] For each W_0, $\bar{R}$ is estimated only over the second half of the simulation, thus, discarding a transient $T_S/2$ for each run.

[27] The width of the hysteric loop remains essentially unchanged when varying N from 200 to 2000.